A Journal of the Gesellschaft Deutscher Chemiker

Angewandte Chemie

GDCh

International Edition

www.angewandte.org

Accepted Article

Title: Sugar-Based Polymers from D-xylose: Living Cascade Polymerization, Tunable Degradation, and Small Molecule Release

Authors: Antonio Rizzo, Gregory I. Peterson, Atanu Bhaumik, Cheol Kang, and Tae-Lim Choi

To be cited as: *Angew. Chem. Int. Ed.* 10.1002/anie.202012544

Link to VoR: https://doi.org/10.1002/anie.202012544

WILEY-VCH

10.1002/anie.202012544

WILEY-VCH

RESEARCH ARTICLE

Sugar-Based Polymers from D-xylose: Living Cascade Polymerization, Tunable Degradation, and Small Molecule Release

Antonio Rizzo,† Gregory I. Peterson,† Atanu Bhaumik,† Cheol Kang, Tae-Lim Choi*

Dedicated to Prof. Bert Meijer on the occasion of his 65th birthday and for his service to J. Polym. Sci., Wiley for 15 years.

Dr. A. Rizzo, Dr. G. I. Peterson, Dr. A. Bhaumik, Dr. C. Kang, Prof. T.-L. Choi
Department of Chemistry
Seoul National University
Seoul 08826, Republic of Korea
E-mail: tlc@snu.ac.kr

† These authors contributed equally.

Supporting information for this article is given via a link at the end of the document

Abstract: Enyne monomers derived from D-xylose underwent living cascade polymerizations to prepare new polymers with a ring-opened sugar and degradable linkage incorporated into every repeat unit of the backbone. Polymerizations were well-controlled and had living character, which enabled the preparation of high molecular weight polymers with narrow molecular weight dispersity values and a block copolymer. By tuning the type of acid-sensitive linkage (hemi-aminal ether, acetal, or ether functional groups), we could change the degradation profile of the polymer and the identity of the resulting degradation products. For instance, the large difference in degradation rates between hemi-aminal ether- and ether-based polymers enabled the sequential degradation of a block copolymer. Furthermore, we exploited the generation of furan-based degradation products, from an acetal-based polymer, to achieve the release of covalently bound reporter molecules upon degradation.

Introduction

Olefin metathesis is a versatile method which has been widely used for the formation of new carbon-carbon bonds in organic synthesis.[1,2] The basic metathesis reactions, ring-opening, ring-closing, and cross metathesis, have also been applied to polymer synthesis, giving ring-opening metathesis polymerization (ROMP),[3-5] cyclopolymerization,[6,7] and acyclic diene metathesis (ADMET) polymerization,[8-10] respectively. With the use of the popular Grubbs-type catalysts, these metathesis polymerizations are generally tolerant to a wide-range of functional and reaction conditions, and therefore, are ideal for preparing well-defined functional polymers for a wide-range of applications.[2,11,12] The use of metathesis polymerizations to prepare fully degradable materials, however, has been relatively under-explored. The development of new degradable polymers has become an important topic as their potential is being realized in various industries.[13-16]

A common strategy to impart degradability to a polymer is to incorporate degradable linkages into the polymer backbone. ADMET polymerization has been utilized to prepare degradable polymers which contain thermally-sensitive or hydrolyzable esters and sulfonate esters,[17-21] acid-sensitive acetals,[22] and enzymatically-cleavable azobenzenes.[23] ROMP has been used to prepare various partially degradable polymers by copolymerization of monomers containing acid-sensitive acetals, ketals, phosphoesters, and silyl ethers,[24-32] base-sensitive esters,[29] and redox/thiol-sensitive disulfides.[27] In many cases, the content of the degradable monomers was limited due to their poor polymerization performance at higher incorporation ratios. Only a few monomers, containing pH-sensitive enol ether,[33] or hemiaminal ether-based linkages,[34-37] have been successfully homopolymerized to achieve fully degradable ROMP polymers. Of note, other metathesis polymers which contain degradable linkages have been prepared,[38-41] but their degradability was not explored.

Degradable polymers have also been prepared via the cascade metathesis polymerization of monomers bearing terminal alkynes and cyclic alkenes (also referred to as tandem ring-closing/ring-opening metathesis polymerization or enyne metathesis polymerization) using the third-generation Grubbs catalyst (G3).[42-46] This cascade metathesis polymerization (**Figure 1A**) was first developed in our group using monomers that do not yield degradable polymers.[47] Mechanistic studies supported that the catalyst first reacts with the alkyne then undergoes intramolecular ring-closing and ring-opening steps (**Figure 1B**).[48] Controlled living polymerizations were observed for monomers with N- and di-substituted C-based linkers (at the X position between the cyclohexene and terminal alkyne, e.g., **1** and **2**; **Figure 1C**), however a monomer with an O linker (**3**) could only be polymerized in a non-controlled fashion at low concentrations (to favor productive intramolecular reactions).[49] Hawker and Gutekunst expanded upon this concept with macrocyclic monomers containing specific amino-acid sequences that could be degraded under transesterification conditions.[44] Gutekunst and coworkers also prepared modular monomers (e.g., **4**) which gave polymers with acid-sensitive acetals in each repeat unit.[46]

10.1002/anie.202012544

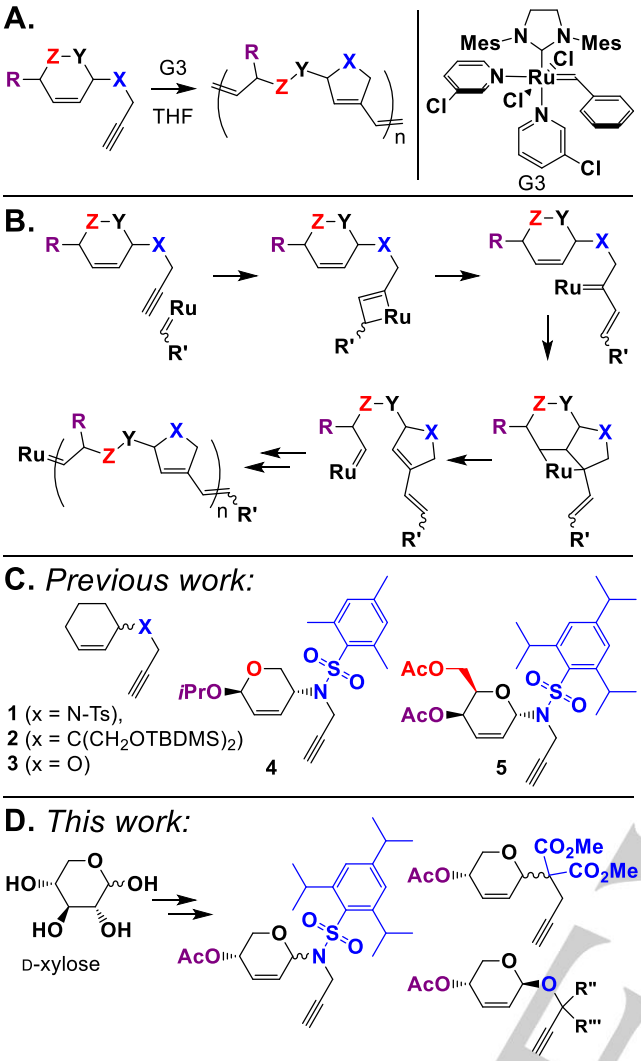

Figure 1. (A) General reaction scheme for the cascade metathesis polymerization of monomers with terminal alkyne and cyclohexene units. (B) Proposed polymerization mechanism. (C) Previous work: representative monomers for cascade metathesis polymerization. (D) In this work: new sugar-based monomers with N, C, and O linkers prepared from D-xylose. Mes = mesityl. TBDMS = tert-butyldimethylsilyl. Ts = tosyl.

We recently reported the cascade metathesis polymerization of sugar-based monomers (SBMs) to yield fully degradable polymers containing acid-sensitive hemiaminal ethers.[45] Specifically, we prepared SBMs from D-galactose and D-glucose with the alkyne attached at the anomeric carbon via a *N*-2,4,6-triisopropylbenzenesulfonyl (*N*-TPS) linker (e.g., **5**). While we could achieve high molecular weight polymers in a controlled and living manner, compared to other cascade polymerizations, the polymerization of these monomers was relatively slow. For example, at room temperature (RT), our best monomer (**5**) reached full conversion in 7 h with a monomer to initiator ratio (M/I) of 100,[45] compared to 30 min for **4** (M/I of 200 and similar concentration),[46] and 1 min for **1** (M/I of 100 and slightly higher concentration).[47] We attributed the slower polymerization rates to the more substituted (sterically crowded) sugar ring. Also, the scope for the SBMs was rather limited because we could only use N-based linkers (at the X position, see **Figure 1**): polymerizations with other linkers failed. We imagined that we might be able to further improve the polymerization performance and expand the diversity of SBMs by switching to monomers, based on D-xylose, with different linkers that could enable the modulation of polymer degradability (**Figure 1D**).

Herein, we report the living polymerization of new SBMs. The switch to D-xylose-based monomers enhanced the polymerization efficiency and enabled the implementation of N-, C- and O-based linkers in the monomer. We, for the first time, were able to obtain controlled living polymerizations with monomers containing O linkers. The linker was also found to play a critical role in tuning the degradability of the resulting polymers and the identity of the degradation products: the later we exploited to trigger the secondary release of a reporter molecule after polymer degradation.

Results and Discussion

Monomers **M1-4** (**Figure 2**) were prepared from the pyranose form of D-xylose (see **Figure S1** in the Supporting Information, SI, for synthetic details). We first explored the polymerization of **M1** (*N*-TPS linker) with G3 catalyst. After optimizing the polymerization conditions (see **Table S1** in the SI), we found that the polymerization was well controlled up to M/I of 125 (**Figure 3A**), with number average molecular weight (M_n) values ranging 10.6 – 38.7 kDa and molecular weight dispersity ($Đ_M$) values ranging 1.11 – 1.40 (**Table 1**, entries 1 – 5). With our previous D-glucose-based monomer with a *N*-TPS linker (which has an additional CH_2OAc group), we could only maintain control of the polymerization up to M/I of 50 due to incomplete conversion and long reaction times (at M/I of 75 and 100, monomer conversions reached 87% in 12 h and 77% in 15 h, respectively).[45] Thus the reduced steric bulk on the sugar ring appeared to significantly enhance the polymerization efficiency (full conversion within 4 h). We conducted a ^{1}H NMR kinetics study and found first order conversion of monomer (see **Figure S2** in the SI), suggesting monomer reacting with the catalyst is rate determining, which is in accord with the previously observed reactivity of D-glucose-based monomers.

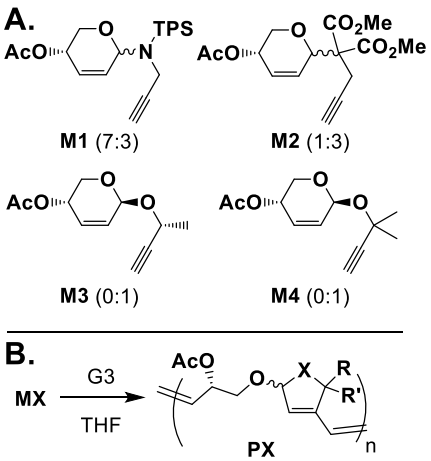

Figure 2. (A) Chemical structures and stereochemistry (α:β) for monomers used in this study. (B) Cascade polymerization of D-xylose-based monomers.

10.1002/anie.202012544

Table 1. Polymerization Results for SBMs (MX).

entry	MX	M/I	conc. (M)[a]	temp. (˚C)[b]	time (h)	conv. (%)[c]	yield (%)	M_n (kDa)[d]	$Đ_M$[d]
1	**M1**	30	0.1	10	1	99	87	10.6	1.11
2	**M1**	50	0.1	10	2	>99	68	18.4	1.17
3	**M1**	75	0.1	10	3	>99	85	25.8	1.21
4	**M1**	100	0.1	10	4	>99	89	31.5	1.32
5	**M1**	125	0.1	10	5.5	>99	87	38.7	1.40
6	**M2**	30	0.1	10	1	>99	76	11.5	1.10
7	**M2**	50	0.1	10	2	>99	84	17.8	1.20
8	**M2**	75	0.1	10	3	>99	86	29.1	1.34
9	**M2**	100	0.1	10	4	96	84	33.2	1.39
10	**M3**	30	0.05	RT	0.33	>99	88	8.9	1.09
11	**M3**	50	0.05	RT	0.5	>99	86	14.4	1.10
12	**M3**	75	0.05	RT	0.75	>99	82	21.3	1.12
13	**M3**	100	0.05	RT	1	97	86	29.0	1.24
14	**M3**	125	0.05	RT	1.33	>99	84	32.2	1.29
15	**M4**	20	0.3	30	0.67	>99	62	7.7	1.15
16	**M4**	30	0.3	30	0.92	>99	65	11.2	1.19
17	**M4**	40	0.3	30	1.25	99	87	18.6	1.22
18	**M4**	50	0.3	30	1.5	98	86	22.4	1.28
19	**M4**	60	0.3	30	2.5	>99	84	25.9	1.27

[a] Monomer concentration. [b] RT = room temperature, which averaged ca. 21 ˚C. [c] Conversion: determined by crude ^{1}H NMR analysis. [d] Determined by size exclusion chromatography (SEC), in THF, calibrated by polystyrene standards.

We next turned our attention to monomers with C-based and O linkers. Using the same optimized polymerization conditions, the polymerization of **M2** (C-$(CO_2Me)_2$ linker) was well controlled up to M/I of 100 (**Figure 3B**), with M_n values ranging 11.5 – 33.2 kDa and $Đ_M$ values ranging 1.10 – 1.39 (**Table 1**, entries 6 – 9). These results are comparable to our previous results with monomers utilizing di-substituted carbon linkers,[49] albeit with longer polymerization times. Again, ^{1}H NMR kinetics studies revealed first order consumption of monomer (see **Figure S2** in the SI). Unfortunately, initial attempts to polymerize monomers with O linkers were not as successful. As mentioned above, polymerization of **3** (**Figure 1C**), which has a simple propargyl group (no additional substituents), was only achieved with dilute conditions and gave low molecular weight polymers with broad dispersity (>1.5).[48,49] Similarly, polymerization of the D-xylose-analogue of this monomer (see **SM1** in the SI) was unsuccessful (see **Table S1,** entry 10 and 11 in the SI). Fortunately, addition of a methyl group adjacent to the alkyne (**M3**) enabled successful polymerization, presumably by sterically shielding the propagating carbene and slowing decomposition pathways.[50] By decreasing the concentration and increasing the temperature, compared to the optimized conditions for **M1** and **M2** (see **Table S1** in the SI for optimization), we found the polymerization of **M3** to be controlled up to M/I of 125 (**Figure 3C**), with M_n values ranging 8.9 – 32.2 kDa and $Đ_M$ values ranging 1.09 – 1.29 (**Table 1**, entries 10 – 14). Addition of a second methyl group (**M4**) led to a rather significant decrease in polymerization performance. However, by increasing the concentration and further increasing the temperature, we could achieve controlled polymerizations up to M/I of 60 (**Figure 3D**), with M_n values ranging 7.7 – 25.9 kDa and $Đ_M$ values ranging 1.15 – 1.28 (**Table 1**, entries 15 – 19). For both of these monomers, kinetics studies supported first order monomer conversion (see **Table S2** in the SI) albeit with slower rates (than **M1** and **M2**), presumably due to the added steric hinderance of the methyl groups, which would slow catalyst approach to the alkyne. Likewise, the polymerization of **M4** (with a dimethyl group) was the slowest by at least one order of magnitude.

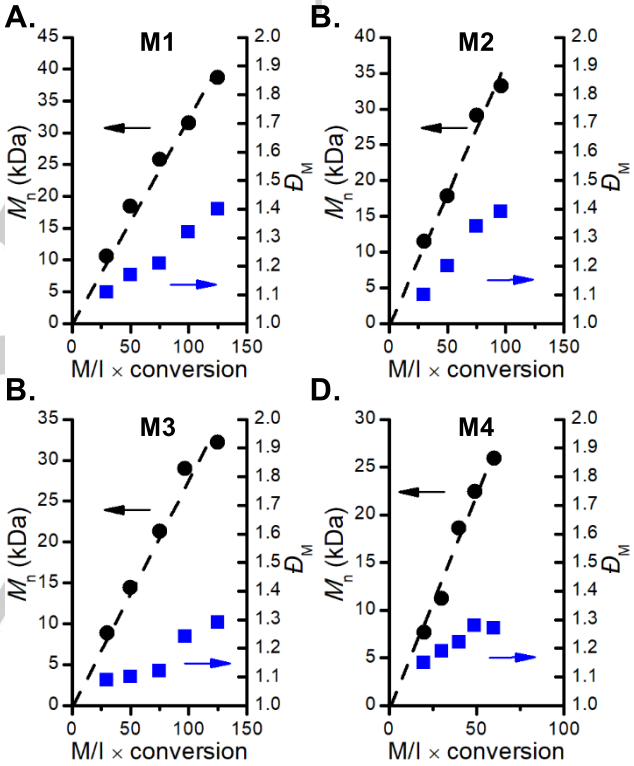

Figure 3. Controlled cascade metathesis polymerization of D-xylose-based monomers. (A) Linear plots of M_n versus M/I × conversion for **M1**, (B) **M2**, (C) **M3**, and (D) **M4**. Black circles represent M_n values. Blue squares represent $Đ_M$ values. Dashed lines are for visual aid only.

To determine the influence of linker type (e.g., N, C, O) on each polymer's degradability and the resulting degradation products, we conducted ^{1}H NMR studies with each polymer in acidic conditions. Specifically, polymers were dissolved in CD_3CN with 2% v/v MeOH, HCl was added, and the degradation was monitored over time. With an HCl concentration of 5×10^{-5} M, **P1** underwent complete degradation to **D1** (**Figure 4A**, degradation products confirmed by NMR and HRMS analysis, see the SI for details) within ca. 4 min (**Figure 4B**). Attempts to further decrease the acid resulted in the incomplete degradation of the polymer (degradation leveled off around 40%). **D1** is structurally

10.1002/anie.202012544

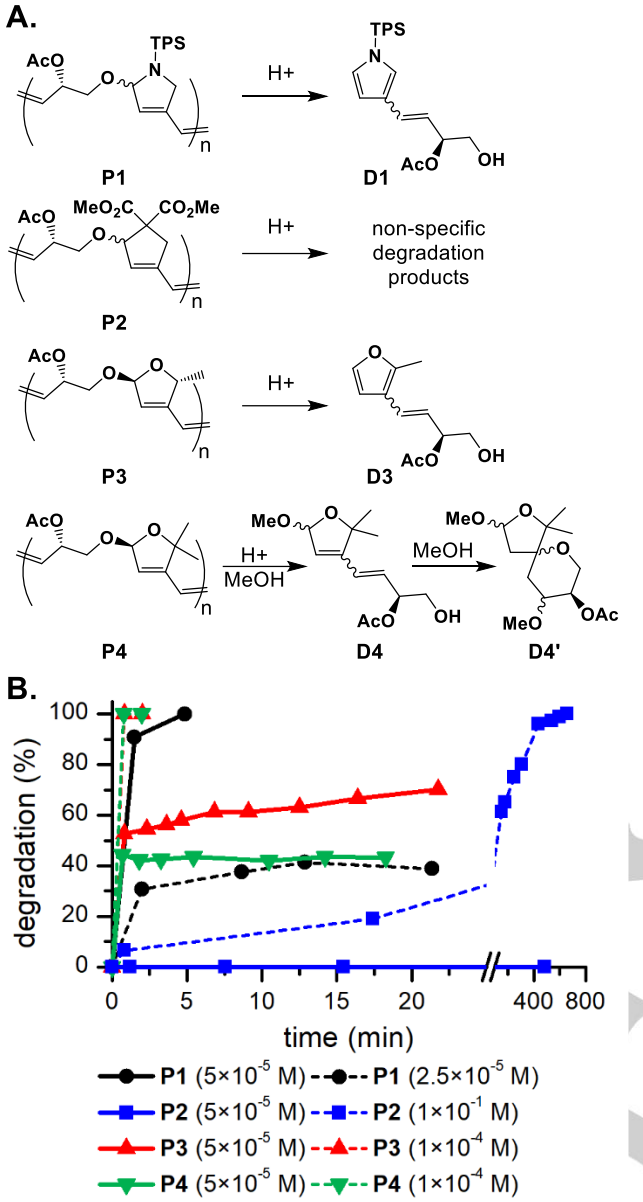

Figure 4. (A) Acidic degradation of polymers and the resulting degradation products. (B) Plot of degradation versus time for **P1** – **P4**. The HCl concentrations are indicated in the legend. Other conditions: polymers at 0.02 M in CD_3CN with 2% v/v MeOH. Solid and dashed lines are for visual aid only.

analogous to the pyrrole-based degradation products observed for our previous D-glucose/galactose-based polymers.[45] **P2** did not degrade over ca. 8 h with an HCl concentration 5×10^{-5} M. Relatively slow degradation was observed at a much higher HCl concentration (1×10^{-1} M), reaching full degradation in 11 h (to non-specific degradation products). **P3** underwent nearly instantaneous degradation to a furan-based product (**D3**) with an HCl concentration of 1×10^{-4} M (degradation leveled off around 60% with an HCl concentration of 5×10^{-5} M). Finally, **P4** also underwent nearly instantaneous degradation (to **D4**) with an HCl concentration of 1×10^{-4} M (although degradation leveled off around 40% with an HCl concentration of 5×10^{-5} M). As the degradation with catalytic amounts of acid should be proton neutral, the observation of the % degradation leveling off (at the lower acid concentrations) suggests consumption of acid via an unknown mechanism. Based on these results, we rank the acidic degradability of polymers as follows: **P1** > **P3** > **P4** > **P2**. While **D1** and **D3** (which contain aromatic pyrrole and furan moieties, respectively) were quite stable (under the degradation conditions), we observed an interesting transformation in which **D4** further degraded to **D4'** via subsequent intermolecular and intramolecular alcohol additions at higher HCl concentrations (e.g., 1×10^{-2} M, see **Figure S30** in the SI for more details). Overall, these studies demonstrate the highly degradable nature of D-xylose-based polymers under mildly acidic conditions. Notably, **P1** and **P2** showed no degradation over 7 d in solution without acid, whereas **P3** and **P4** showed some slow degradation, reaching ca. 15 and 9% degradation in 7 d without acid, respectively (see **Figure S3**).

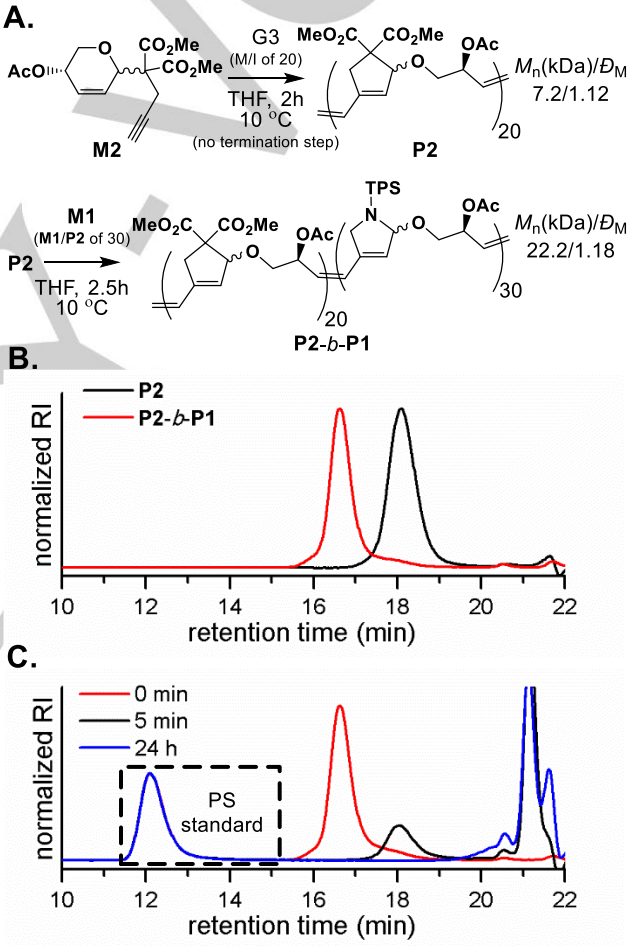

Figure 5. (A) Synthetic scheme for the preparation of **P2**-*b*-**P1**. (B) SEC traces for **P2** (via an aliquot just before addition of **M1**) and **P2**-*b*-**P1**. Peaks normalized to the maximum peak height. (C) SEC traces at various time points during the acidic degradation of **P2**-*b*-**P1** in THF (HCl concentration of 1.3 M). Peaks normalized to an internal standard (ca. 900 kDa polystyrene, PS).

Next, we wanted to explore the feasibility of preparing a block copolymer (from two different SBMs) and achieve sequential degradation of blocks with very different degradation profiles. In our previous report,[45] we could not demonstrate sequential degradation because polymers from D-glucose and D-galactose showed similar degradation rates due to their structural

10.1002/anie.202012544

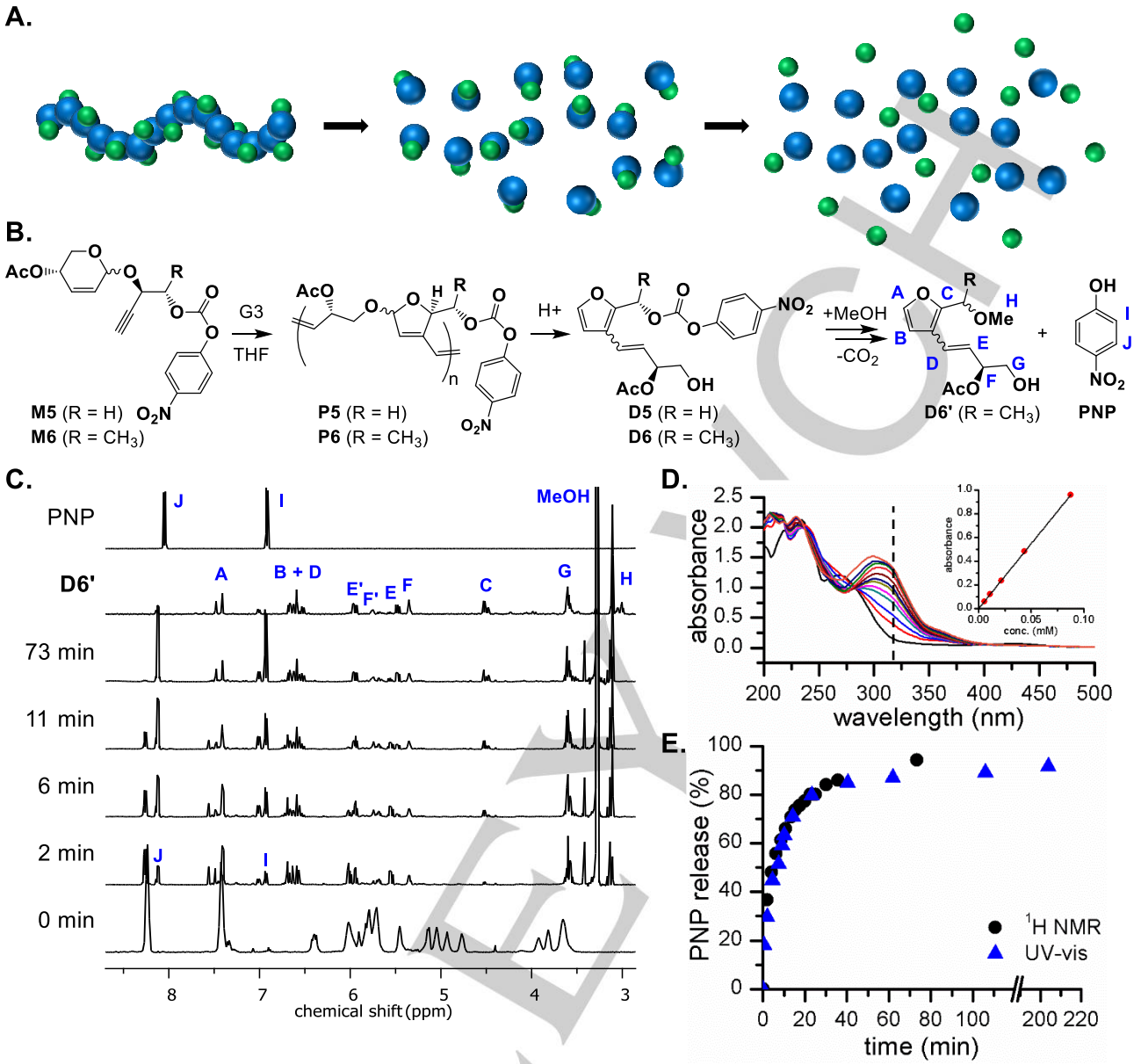

Figure 6. (A) Scheme for the degradation of a polymer and release of molecular cargo. (B) Synthesis and degradation of **P5** and **P6** with release of PNP. Blue letters represent protons assigned in the ^{1}H NMR spectrum. (C) Stacked ^{1}H NMR spectrum of **P6** undergoing acidic degradation (1×10^{-3} M HCl concentration in CD_3CN with 2% v/v MeOH). (D) Change in UV-vis absorbance during the acidic degradation of **P6** (1×10^{-3} M HCl concentration in CH_3CN with 2% v/v MeOH). The inset plot shows the PNP calibration curve (absorbance at 320 nm) used to determine the concentration of released PNP. (E) Plot of the percentage of PNP released from **P6** over time for ^{1}H NMR and UV-vis experiments.

similarity. We began by first polymerizing **M2**, and then adding **M1** to the **P2** block (with a living chain end, M_n: 7.2 kDa and $Đ_M$: 1.12) to form **P2**-*b*-**P1** (**Figure 5A**). Comparison of the SEC traces from the block copolymer and first block revealed a clear shift in the SEC peak to shorter retention times (M_n: 22.2 kDa, **Figure 5B**), without residual **P2** block or excessive tailing, and maintaining a $Đ_M$ of 1.18. This result supports the living nature of the cascade metathesis polymerization. With this block copolymer on hand, we began to explore its acidic degradation. The polymer was dissolved in THF, HCl was added (final concentration of 1.3 M), and the degradation was monitored by SEC (**Figure 5C**). After 5 min, the **P1** block was completely degraded, leaving only the **P2** block having the same M_n as the **P2** intermediate in the block copolymer synthesis (see **Figure S4** and **S5** in the SI, which show the overlapped SEC traces of the **P2** blocks, from synthesis and degradation, and the loss of all **P1** signals after 5 min by ^{1}H NMR spectroscopy, respectively). After 24 h, the **P2** block too was almost completely degraded to small molecules, with only a little oligomeric material remaining. Therefore, sequential degradation of a block copolymer was achieved. This result highlights further highlights the advantage of broadening the monomer scope, and thereby, being able to tune polymer degradability.

In most cases, the degradation of D-xylose-based polymers yielded well-defined small molecules such as pyrroles (**D1**), furans (**D3**) and even spirocyclic compounds (**D4'**). This inspired us to explore the feasibility of designing a functional degradation

compound and proceeding backward by retrosynthetic analysis to a new monomer. Furan-maleimide Diels-Alder adducts have been shown to function as thermal or mechanochemical triggers for initiating depolymerization or releasing small molecules, respectively.[51,52] In these examples, the generation of a furfuryl carbonate intermediate, which undergoes further decomposition via CO_2 loss and production of a carbocation intermediate, was the key to the desired reactivity. With this specific reactivity in mind, we designed a furfuryl carbonate degradation product (an analogue to **D3**) which would enable the release of covalently bound molecular cargo, after the acidic degradation of the polymer. Polymers that release cargo upon degradation (**Figure 6A**) are relevant to various applications including sensing, self-healing, and drug delivery.[16,53-56] We designed two new monomers, **M5** and **M6** (see **Figure S6** in the SI for synthetic details), such that their polymers (**P5** and **P6**) would generate **D5** and **D6**, which would subsequently release *p*-nitrophenol (PNP) as a model cargo molecule (**Figure 6B**), which could be easily monitored by UV-vis and NMR analysis. Each monomer underwent efficient polymerization at a M/I of 30 (0.05 M monomer concentration at RT), giving polymers with M_n ($Đ_M$) of 8.6 kDa (1.17) and 9.7 kDa (1.12) for **P5** and **P6**, respectively.

We first studied the degradation and PNP release for **P5**. Based on density functional theory (DFT) calculations and experimentally measured half-lives of model compounds conducted by Robb and coworkers,[52] we expected that PNP release would be considerably slow for this polymer. Indeed, we observed rapid degradation of the polymer to **D5** upon addition of HCl at RT (1×10^{-3} M HCl concentration in CD_3CN with 2% v/v MeOH), however, only 13% of PNP released over 31 h via methanolysis (see **Figure S7** in the SI). Robb and coworkers also found that addition of an α-methyl group was found to lower the activation barrier of furfuryl carbonate decomposition and enable release to occur at relatively fast rates at RT, presumably due to higher stabilization of the furfuryl cationic intermediate at the secondary carbon (see **Figure S8** in the SI).[52] Therefore, we expected **P6** to exhibit much faster release of PNP. Subjecting **P6** to the same acidic degradation conditions, we observed, with both ^{1}H NMR (**Figure 6C** and **6E**) and UV-vis (**Figure 6D** and **6E**) experiments, that rapid and complete degradation of the polymer to **D6** initially occurred in less than 2 min, followed by the fast secondary release of PNP (>90% in less than 2 h). Formation of the degradation product **D6'** (via trapping the cationic intermediate with MeOH, see **Figure S8** in the SI) supports that the PNP was released via the furfuryl intermediate, rather than simple methanolysis, which is a much slower process. Notably, **P6** showed better stability in solution without acid than **P3** (over 10 d, see **Figure S9** in the SI), as we observed no polymer degradation and only ca. 1.2% loss of PNP via methanolysis. Furan derivatives are known to have a broad range of biological activity (as are pyrroles),[57-59] which should be taken into consideration when identifying applications for these materials. Overall, these results demonstrate that reactivity of the SBP degradation products can be exploited for the release of molecular cargo.

Conclusion

We have expanded the scope of the cascade metathesis polymerization of SBM, by switching to a monomer design based on D-xylose with different linkers, to produce new fully degradable polymers. Polymerizations were well-controlled and high molecular weights were obtained (M_n up to ca. 39 kDa) with generally narrow dispersity (1.09−1.40). The living nature of the polymerization was supported by the preparation of a block copolymer from SBMs with two different linker types (N- and C-based linkers in **M1** and **M2**, respectively). The resulting block copolymer contained a first block with hemi-aminal ether functional groups and a second block with ether functional groups. The significantly slower degradation of the ether functionalities (compared to the hemi-aminal ethers) enabled sequential degradation of the block copolymer under acidic conditions. The linker also influenced the resulting degradation products. We took advantage of the reactivity of furan-based degradation products to prepare polymers which undergo initial acidic degradation, followed by secondary release of molecular cargo. We envision these polymers may have potential use in the various arenas which require degradable polymers or small molecule release capabilities (e.g., drug delivery, sensors, etc.).

Supporting Information: Supplemental figures, experimental details, and characterization of monomers, polymers, and degradation products are included in the SI.

Acknowledgements

We acknowledge Hojoon Song (SNU) for help with monomer scaleup. The authors also thank the Korean NRF for the following funding: Creative research initiative and Young Investigator Grant (NRF-2018R1C1B6003054).

Keywords: polymerization • metathesis • cascade • degradation • sugars

[1] R. H. Grubbs in *Handbook of Metathesis, Vols. 1, 2*; Wiley-VCH: Weinheim, **2003**.
[2] O. M. Ogba, N. C. Warner, D. J. O'Leary, R. H. Grubbs. *Chem. Soc. Rev.* **2018**, *47*, 4510-4544.
[3] C. W. Bielawski, R. H. Grubbs. *Prog. Polym. Sci.* **2007**, *32*, 1-29.
[4] R. R. Schrock. *Acc. Chem. Res.* **1990**, *23*, 158-165.
[5] O. Nuyken, S. D. Pask. *Polymers* **2013**, *5*, 361-403.
[6] G. I. Peterson, S. Yang, T.-L. Choi. *Acc. Chem. Res.* **2019**, *52*, 994-1005.
[7] M. R. Buchmeiser. *Polym. Rev.* **2017**, *57*, 15-30.
[8] P. Atallah, K. B. Wagener, M. D. Schulz. *Macromolecules* **2013**, *46*, 4735-4741.
[9] H. Mutlu, L. M. de Espinosa, M. A. R. Meier. *Chem. Soc. Rev.* **2011**, *40*, 1404-1445.
[10] L. Caire da Silva, G. Rojas, M. D. Schulz, K. B. Wagener. *Prog. Polym. Sci.* **2017**, *69*, 79-107.
[11] C. Slugovc. Industrial Applications of Olefin Metathesis Polymerization in *Olefin Metathesis: Theory and Practice*; Grela, K. Ed.; John Wiley & Sons, Inc.: Hoboken, New Jersey, **2014**, pp. 329-333.
[12] K. D. Camm, D. E. Fogg. From Drug Cocktails to Tissue Engineering: Synthesis of ROMP Polymers for Biomedical Applications in *Metathesis Chemistry. NATO Science Series, vol 243;* Imamoglu Y., Dragutan V., Karabulut S. Eds.; Springer: Dordrecht, Netherlands, **2007**, pp. 285-303.
[13] B. Jothimani, B. Venkatachalapathy, N. S. Karthikeyan, C. Ravichandran. A Review on Versatile Applications of Degradable Polymers in *Green Biopolymers and their Nanocomposites*;

Gnanasekaran, D., Ed.; Springer Singapore: Singapore, **2019**, pp. 403-422.
[14] R. P. Brannigan, A. P. Dove. *Biomater. Sci.* **2017**, *5*, 9-21.
[15] Y. Cao, K. E. Uhrich. *J. Bioact. Compatible Polym.* **2019**, *34*, 3-15.
[16] R. E. Yardley, A. R. Kenaree, E. R. Gillies. *Macromolecules* **2019**, *52*, 6342-6360.
[17] A. Lv, Y. Cui, F.-S. Du, Z.-C. Li. *Macromolecules* **2016**, *49*, 8449-8458.
[18] R. R. Parkhurst, S. Balog, C. Weder, Y. C. Simon. *RSC Adv.* **2014**, *4*, 53967-53974.
[19] P. A. Fokou, M. A. R. Meier. *J. Am. Chem. Soc.* **2009**, *131*, 1664-1665.
[20] W. C. Shearouse, L. M. Lillie, T. M. Reineke, W. B. Tolman. *ACS Macro Lett.* **2015**, *4*, 284-288.
[21] L. M. Lillie, W. B. Tolman, T. M. Reineke. *Polym. Chem.* **2017**, *8*, 3746-3754.
[22] S. D. Khaja, S. Lee, N. Murthy. *Biomacromolecules* **2007**, *8*, 1391-1395.
[23] H. Mutlu, C. Barner-Kowollik. *Polym. Chem.* **2016**, *7*, 2272-2279.
[24] C. Fraser, M. A. Hillmyer, E. Gutierrez, R. H. Grubbs. *Macromolecules* **1995**, *28*, 7256-7261.
[25] D. Moatsou, A. Nagarkar, A. F. M. Kilbinger, R. K. O'Reilly. *J. Polym. Sci., Part A: Polym. Chem.* **2016**, *54*, 1236-1242.
[26] T. Steinbach, E. M. Alexandrino, F. R. Wurm. *Polym. Chem.* **2013**, *4*, 3800-3806.
[27] C.-C. Chang, T. Emrick. *Macromolecules* **2014**, *47*, 1344-1350.
[28] P. Shieh, H. V. T. Nguyen, J. A. Johnson. *Nat. Chem.* **2019**, *11*, 1124–1132.
[29] F. O. Boadi, J. Zhang, X. Yu, S. R. Bhatia, N. S. Sampson. *Macromolecules* **2020**, *53*, 5857–5868.
[30] X. Sui, T. Zhang, A. B. Pabarue, L. Fu, W. R. Gutekunst. *J. Am. Chem. Soc.* **2020**, *142*, 12942–12947.
[31] B. R. Elling, J. K. Su, Y. Xia. *ACS Macro Lett.* **2020**, *9*, 180-184.
[32] P. Shieh, W. Zhang, K. E. L. Husted, S. L. Kristufek, B. Xiong, D. J. Lundberg, J. Lem, D. Veysset, Y. Sun, K. A. Nelson, D. L. Plata, J. A. Johnson. *Nature* **2020**, *583*, 542-547.
[33] J. D. Feist, Y. Xia. *J. Am. Chem. Soc.* **2020**, *142*, 1186-1189.
[34] J. M. Fishman, L. L. Kiessling. *Angew. Chem. Int. Ed.* **2013**, *52*, 5061-5064.
[35] J. M. Fishman, D. B. Zwick, A. G. Kruger, L. L. Kiessling. *Biomacromolecules* **2019**, *20*, 1018-1027.
[36] A. Mallick, Y. Xu, Y. Lin, J. He, M. B. Chan-Park, X.-W. Liu. *Polym. Chem.* **2018**, *9*, 372-377.
[37] T. Debsharma, F. N. Behrendt, A. Laschewsky, H. Schlaad. *Angew. Chem. Int. Ed.* **2019**, *58*, 6718-6721.
[38] Y. Peng, J. Decatur, M. A. R. Meier, R. A. Gross. *Macromolecules* **2013**, *46*, 3293-3300.
[39] E. J. Enholm, K. Mondal. *Synlett* **2009**, *15*, 2539-2541.
[40] J. A. Nowalk, C. Fang, A. L. Short, R. M. Weiss, J. H. Swisher, P. Liu, T. Y. Meyer. *J. Am. Chem. Soc.* **2019**, *141*, 5741-5752.
[41] R. M. Weiss, A. L. Short, T. Y. Meyer. *ACS Macro Lett.* **2015**, *4*, 1039-1043.
[42] G. I. Peterson, T.-L. Choi. *Chem. Sci.* **2020**, *11*, 4843-4854.
[43] J. Yuan, W. Wang, Z. Zhou, J. Niu. *Macromolecules* **2020**, *53*, 5655-5673.
[44] W. R. Gutekunst, C. J. Hawker. *J. Am. Chem. Soc.* **2015**, *137*, 8038-8041.
[45] A. Bhaumik, G. I. Peterson, C. Kang, T.-L. Choi. *J. Am. Chem. Soc.* **2019**, *141*, 12207-12211.
[46] L. Fu, X. Sui, A. E. Crolais, W. R. Gutekunst. *Angew. Chem. Int. Ed.* **2019**, *58*, 15726-15730.
[47] H. Park, T.-L. Choi. *J. Am. Chem. Soc.* **2012**, *134*, 7270-7273.
[48] H. Park, H.-K. Lee, T.-L. Choi. *J. Am. Chem. Soc.* **2013**, *135*, 10769-10775.
[49] H. Park, E.-H. Kang, L. Müller, T.-L. Choi. *J. Am. Chem. Soc.* **2016**, *138*, 2244-2251.
[50] E.-H. Kang, S. Y. Yu, I. S. Lee, S. E. Park, T.-L. Choi. *J. Am. Chem. Soc.* **2014**, *136*, 10508-10514.
[51] B. Fan, J. F. Trant, G. Hemery, O. Sandre, E. R. Gillies. *Chem. Commun.* **2017**, *53*, 12068-12071.
[52] X. Hu, T. Zeng, C. C. Husic, M. J. Robb. *J. Am. Chem. Soc.* **2019**, *141*, 15018-15023.
[53] F. Seidi, R. Jenjob, D. Crespy. *Chem. Rev.* **2018**, *118*, 3965-4036.
[54] M. E. Roth, O. Green, S. Gnaim, D. Shabat. *Chem. Rev.* **2016**, *116*, 1309-1352.
[55] S. T. Phillips, J. S. Robbins, A. M. DiLauro, M. G. Olah. *J. Appl. Polym. Sci.* **2014**, *131*, 40992.
[56] G. I. Peterson, M. B. Larsen, A. J. Boydston. *Macromolecules* **2012**, *45*, 7317-7328.
[57] É. Lukevits, L. Demicheva. *Chem. of Heterocycl. Compd.* **1993**, *29*, 243-267.
[58] L. A. Peterson. *Chem. Res. Toxicol.* **2013**, *26*, 6-25.
[59] R. Kaur, V. Rani, V. Abbot, Y. Kapoor, D. Konar, K. Kumar. *J. Pharm. Chem. Chem. Sci.* **2017**, *1*, 17-32.

10.1002/anie.202012544

Entry for the Table of Contents

Xylose-Derived Polymers

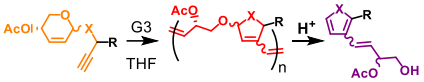

X = N,O, or C linkers

-controlled polymerizations
-fully degradable and tunable
-small molecule release capabilities

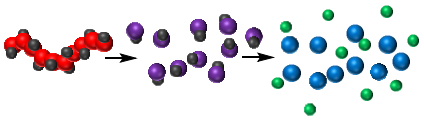

Degradable sugar-based polymers are prepared with cascade metathesis polymerizations in a controlled and living manner. The resulting polymers are fully degradable and degradation profiles can be modified by using different monomer linkers. Polymers can also be designed such that their degradation products undergo secondary reactions to release small molecules.